# Frequency Response Measurements of High-Frequency Linear Systems by Least Squares Identification Techniques

*Kou-Hung Loh*
Department of Electrical Engineering
Texas A&M University
College Station, Texas 77843
U.S.A.

*Randall L. Geiger*
Electrical Engineering and
Computer Engineering Department
Iowa State University
Ames, Iowa 50011

## Abstract

A time–domain least squares system identification algorithm is discussed which is used to calculate frequency responses of linear continuous-time systems with sinusoidal excitations. Both simulation and experimental results have demonstrated that the proposed frequency response measuring technique can tolerate considerable measurement noise as well as significant impurities of excitation signal.

## Introduction

Measurement of the frequency response of a linear continuous-time system is a crucial task for determining the system transfer function[1]. Traditional approaches usually require high precision circuits to perform either direct measurements such as analog peak/phase detectors, or indirect measurements which collect time-domain samples for further interpretation. Both approaches have been found plagued by increasingly erroneous measurements at high frequencies[4]. In this paper, a simple method to determine the gain and phase responses of an unknown linear system based on time-domain samples is proposed. Instead of grabbing a large number of consecutive samples, this new method uses only randomly, asynchronously sampled finite-consecutive data sets which are obtained by fast-tracking, low-to-medium resolution sample-and-hold amplifiers and slow analog-to-digital converters (ADCs). The tight specifications of fast ADCs or analog peak/phase detectors are thus relieved. Simulation and experimental results have shown that the proposed algorithm can accurately measure the frequency responses even with noisy/low-resolution data. This technique is believed to provide a feasible solution to the performance measuring system for supporting high-precision filter tunings[4].

## Background

Consider an unknown linear continuous-time system $T(s)$ excited by a sinusoidal input signal

$$x(t) = V_{im} cos(\omega_0 t) \tag{1}$$

The steady-state response at the output node is represented by

$$y(t) = GV_{im}cos(\omega_0 t + \theta) \tag{2}$$

where $G$ and $\theta$ are known as the gain response and phase response, respectively, at frequency $\omega_0$. The transfer function $T(s)$ evaluated at $s = j\omega_0$ is thus given by

$$T(j\omega_0) = Ge^{j\theta} \tag{3}$$

By applying a basic trigonometric identity to (2), the following equation can be obtained:

$$\begin{aligned} y(t) &= GV_{im}cos(\omega_0 t + \theta) \\ &= GV_{im}(cos(\omega_0 t)cos\theta - sin(\omega_0 t)sin\theta)) \end{aligned} \tag{4}$$

If we sample $x(t)$ at $t = t_0$ and $t = t_0 - T$, and sample $y(t)$ at $t = t_0$, then by adding and subtracting a dummy term into (4), we can derive $y(t_0)$ as follows:

$$\begin{aligned} y(t_0) &= GV_{im}(cos(\omega_0 t_0)cos\theta + \frac{sin\theta}{sin(\omega_0 T)}cos(\omega_0 t_0)cos(\omega_0 T)) \\ &\quad -GV_{im}(sin\theta sin(\omega_0 t_0) + \frac{sin\theta}{sin(\omega_0 T)}cos(\omega_0 t_0)cos(\omega_0 T)) \\ &= G(cos\theta + sin\theta cot(\omega_0 T))V_{im}cos(\omega_0 t_0) - G(\frac{sin\theta}{sin(\omega_0 T)})V_{im}cos(\omega_0(t_0 - T)) \end{aligned} \tag{5}$$

A linear relationship between output sample, $y(t_0)$, and input samples, $x(t_0)$ and $x(t_0 - T)$, thus follows

$$y(t_0) = b_0 x(t_0) + b_1 x(t_0 - T) \tag{6a}$$

where

$$b_0 = G(cos\theta + sin\theta cot(\omega_0 T)) \tag{6b}$$

$$b_1 = -G(\frac{sin\theta}{sin(\omega_0 T)}) \tag{6c}$$

Note that (6a) is valid for all $t_0$ on the real axis provided that $\omega_0 T \neq l\pi$ for all integers $l$. Equation (6a) relates discrete uniformly-spaced time-domain samples of continuous-time waveforms. It is often more common to denote these samples as sequences by the expression

$$y(k) = b_0 x(k) + b_1 x(k - 1) \tag{7}$$

Equation (7) is also known as a first-order moving average (MA) model. Taking the Fourier Transformation on (6a), we can derive

$$Ge^{j\theta} = b_0 + b_1 e^{-j\omega_0 T} \tag{8}$$

Our goal is to determine $G$ and $\theta$. It follows from (8) that $G$ and $\theta$ can be readily obtained if $b_0$ and $b_1$ are known. To measure the frequency response of a linear system with sinusoidal excitation, we need to measure two different "sets" of time-domain

samples to solve for $b_0$ and $b_1$ from two linear equations established by (6a). If there is no error in the measurements, a set of exact solution as given in (6b) and (6c) should be obtained. In case the measurements are contaminated by noise, a greater number of different "sets" can be used to perform least-squares algorithms [2,3], to find $b_0$ and $b_1$. Both gain and phase responses can be subsequently derived from (8).

The frequency response measurement method is not limited to applying a first-order MA model as (7). A higher-order model may also be used in a more general case, which requires at least $N \geq n + m + 1$ sample sets, given by a measurement system for supporting high-precision filter tunings.

$$y(k) = \sum_{i=1}^{n} a_i y(k-i) + \sum_{l=0}^{m} b_j x(k-l) \tag{9}$$

As before, a least-squares algorithm can be used to determine the $\{a_i\}$ and $\{b_j\}$ coefficients in (9) if a sinusoidal excitation is applied. The tradeoff is that more consecutive samples are required in a "set" of data which establishes (9) for the least-squares algorithm.. The frequency response at $\omega_0$ can thus be obtained by

$$Ge^{j\theta} = \frac{\sum_{l=0}^{m} b_l e^{-jl\omega_0 T}}{\sum_{i=1}^{n} a_i e^{-ji\omega_0 T}} \tag{10}$$

The magnitude and phase of the system transfer function at the frequency of the sinusoidal excitation frequency are directly determined from (10). It is interesting to note that the difference equation of (9) is functionally identical to a difference equation which characterizes the system at all frequencies. It follows from (10) that

$$H(z^{-1})|_{z=e^{j\omega_0 T}} = Ge^{j\theta} \tag{11}$$

If one now defines the $z$-domain rational function from the "$a$" and "$b$" coefficients identified from the sinusoidally excited system characterized by (11), we obtain the $z$-domain rational function which agrees with $Ge^{j\theta}$ at $\omega = \omega_0$. This is depicted graphically in Fig.1.

A major difference between the least-squares frequency response measurement and the least-squares system identification is that the former allows undersampling (i.e., sampling at sub-Nyquist rate) of the sinusoidal excitation while the latter only takes oversampled data to avoid aliasing problems. The latter, moreover, usually requires a much "richer" excitation which is usually a band-limited signal.

The measurement system structure based upon the first-order MA model described in (7) is depicted in Fig.2. The structure consists of three fast-aperturing, low-jitter track-and-hold amplifiers to sample the time-domain data on both the input and output of a continuous-time linear system, a precise sinusoidal generator to excite the system. a low-speed, low-to-medium resolution ADC to convert the analog samples, a memory module to store the data and a digital controller to coordinate the data collecting mechanism. All three track-and-hold amplifiers, during most of the

time of their operations, are in the "tracking" mode. When the input/output signals are well tracked, the controller first issues a hold command which generate two clocks $\phi_1$ and $\phi_2$, spaced by a period $T$, to get two consecutive samples at the input and one correlated sample at the output, namely $x(k)$, $x(k-1)$ and $y(k)$, with the track-and-hold amplifiers. The samples are converted to digital data which are stored into the memory module. The amplifiers are then set back to their tracking mode again. This process is repeatedly performed until ample sampled data sets are acquired. Note that, under this mechanism, $k$ can be arbitrary integers and are therefore not limited to consecutive integers since the analog-digital conversions are not necessarily real-time operations. Once sufficient samples are obtained, the system host begins calculating the coefficients $b_0$ and $b_1$ in (8) by solving the least–squares linear equations

$$\hat{\mathbf{W}}^T = [\mathbf{X(k)}^T\mathbf{X(k)}]^{-1}[\mathbf{X(k)}^T y(\mathbf{k})] \tag{12}$$

where $\hat{\mathbf{W}} = [b_0, b_1]^T$, $\mathbf{X(k)} = [x(\mathbf{k}), x(\mathbf{k}-1)]^T$, $\mathbf{k} = [k_1, k_2, ..., k_N]^T$ where $N$ is the dimension of $\mathbf{k}$, and $k_i$'s are arbitrary real numbers denoting when each sample set is to begin which in real-time identification problems are chosen to be successive integers, and $x(\mathbf{k})$ and $y(\mathbf{k})$ are vectors of the sampled input and output, and $x(\mathbf{k}-1)$ is a vector of the late sampled input, with a dimension $N$.

The solutions obtained from (12) can thus be used to compute the gain and phase responses of the continuous-time system at frequency $\omega_0$.

To simulate the proposed frequency response measurement scheme, a 2nd–order bandpass filter with a selectivity of 10 has been chosen as the typical linear system. The system is excited by a frequency at its resonant frequency. The amplitude of the sinusoidal is set to unity. The signal nonideality of the excitation is approximated by a second harmonic sinusoid with a nominal amplitude of 0.01. Other system nonidealities including quantization errors, measurement noise, system noise and the timing mismatch/uncertainty are simplified into random sequences uniformly distributed in (-0.01,0.01) added to both input and output measurements. The first–order least–squares algorithm, as presented in (12), is used to solve coefficients $b_0$ and $b_1$. The simulation results are shown in Figs.3-6. Several observations can be made based upon these results. First, the measurement results become more and more accurate as the dimension $N$ increases. This can be best verified by observing the standard deviation of the measurements. Second, the measuring structure is able to tolerate fairly noisy environments (as low as 20dB SNR) while still maintaining 1% accuracy. Finally, as shown in Figs.4.5 and 4.6, it is observed that the total harmonic distortion(THD) of the excitation signal has little impact on the measurement accuracy unless the sinusoidal excitation is severely distorted. All statistics shown in simulation results are calculated from 100 independent trials.

## Experimental Results

The experimental prototype structure of the proposed measurement scheme is shown in Fig.7. In Fig.8(a), gain responses of a 2nd-order bandpass filter with $Q \approx 10$ obtained at 30 uniformly–spaced frequencies by the proposed measurement scheme (marked by 'O'), are compared with other measurements. One hundred sets of samples

were acquired for each excitation frequency by the HP54111 and were then used to calculate the first–order least-squares solutions. The sampling frequency was set to $2.5MHz$. The excitation amplitude was set to $1V_{pp}$, and the maximal measurable ranges of both input and output channels were fixed at $1.28V$. The solid line was measured by the HP3585A, while 'X' markers were measured directly from HP54111 after 64 times of waveform averaging. The measurement difference between the two instruments was due to their different input capacitance and the imperfectness of the filter buffer circuits. The phase response measurement results of the 2nd-order bandpass filter are presented in Fig.8(b). The absolute measured difference for both gain and phase are given in Fig.8(c) in which one can observe the gain errors and phase errors are, in general, below 1% and 2 degrees, respectively. Note that the raw samples used in the least-squares calculation have less than 6-bit accuracy. The same measurement algorithm was used to measure the frequency response of a 2nd-order lowpass notch filter. The results are given in Figs.9(a) and 9(b) in which both gain and phase measurements show relatively larger errors around the notch frequency. This problem can be partially overcome by dynamically scaling the input measurement range of the ADC and consequently achieving better resolutions.

## Conclusions

We have developed a new frequency response measurement scheme which is feasible for high-frequency, monolithic implementations. Instead of using state-of-the-art high-frequency analog peak/phase detectors or high-speed ADCs, the structure exploits only fast-aperturing track-and-hold amplifiers as the front-end circuits. From extensive simulations, the algorithm has proven to be insensitive to harmonic distortion of the input and noise unless the sampled data are badly contaminated. With 6-bit resolution samples, the experimental results have shown the algorithm can effectively measure the gain and phase responses with 1% and 2-degree accuracies, respectively. Further improvements of the accuracy are readily available by implementing higher-resolution and dynamically scalable ADC.

## References

[1] K.H.Loh, D.L.Hiser, W.J.Adams and R.L.Geiger, "A Versatile, Digitally Controlled Continuous-Time Filter Structure with Wide-Range and Fine-Resolution Programmability", submitted to *IEEE Transactions on Circuits and Systems*, under reviewed.

[2] N.K.Sinha and B. Kuszta, "Modeling and Identification of Dynamic Systems", Ch.3, Van Nostrand Reinhold Company, 1983

[3] V.Strejc, "Least Squares Parameter Estimation", Automatica, pp.535-550, vol.16, no.5, September 1980.

[4] C. Yu, et. al., "Iterative Least Squares Method for Identification of Continuous-time Systems". *Proc. IEEE International Symposium on Circuits and Systems*, Singapore, June 1991

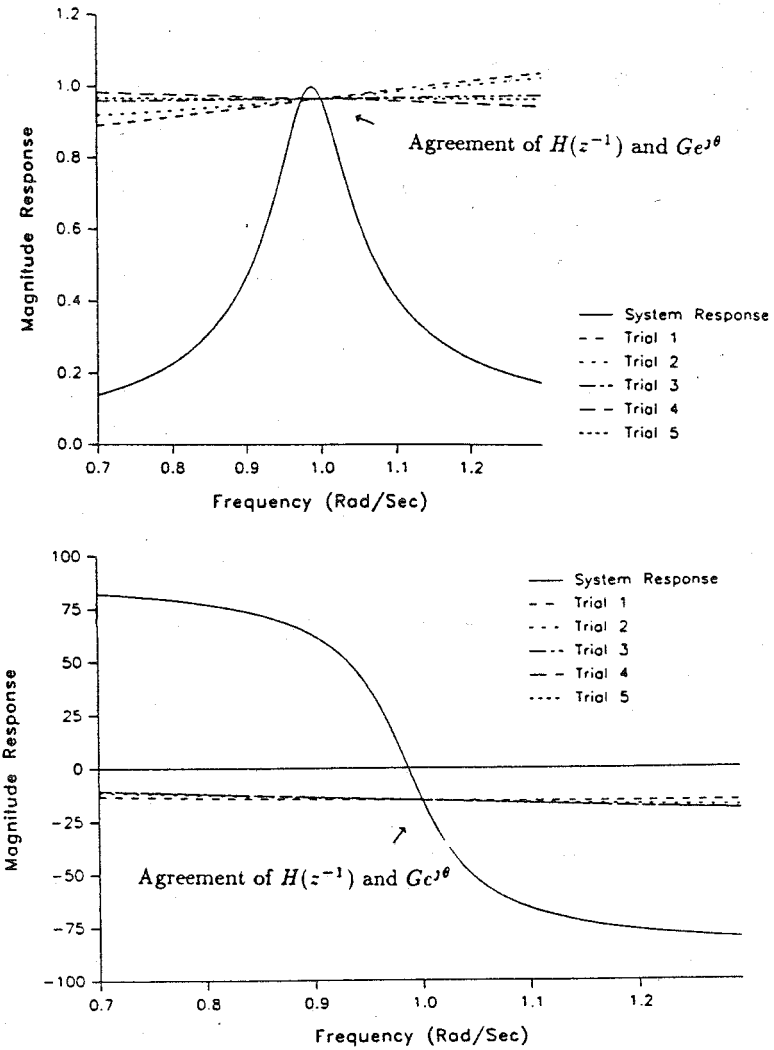


Fig.1 Frequency Response Identified with First-Order Models: (a) Magnitude Response, (b) Phase Response

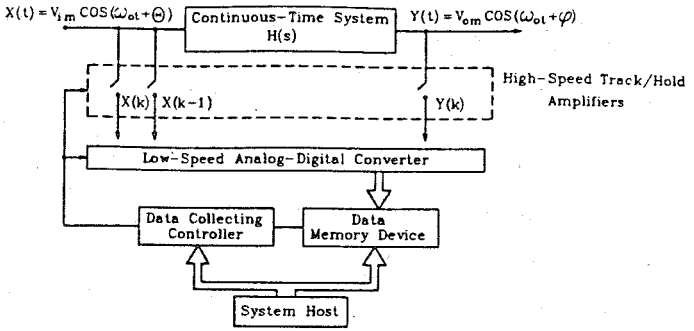


Fig.(2) The proposed Measurement System Architecture

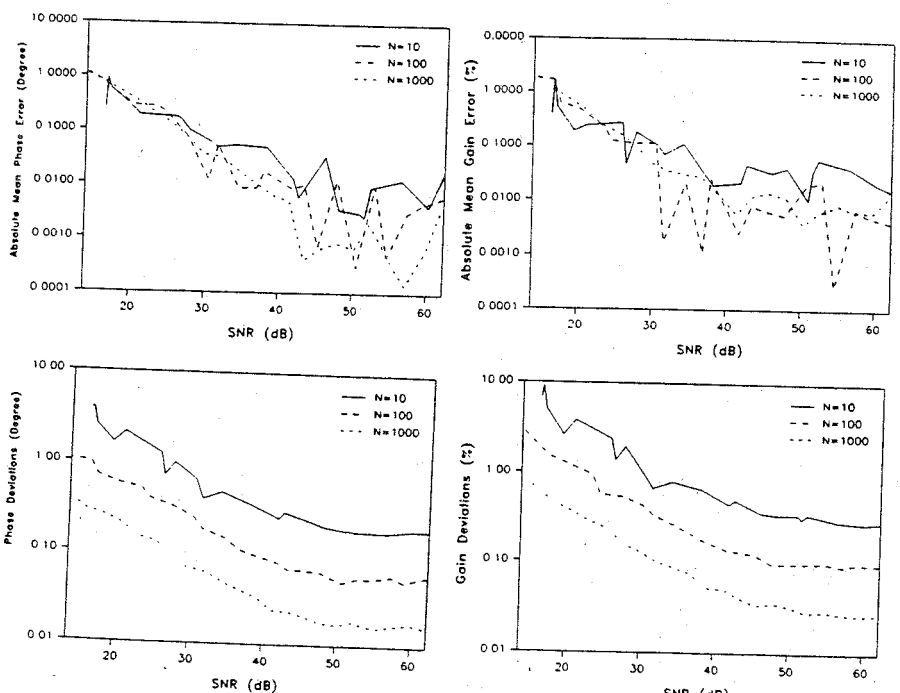


Fig.(4) Monte Carlo Simulation of the Phase Response vs. Signal-Noise Ratio: (a) Phase Error, (b) Standard Deviation of (a)

Fig.(3) Monte Carlo Simulation of the Magnitude Response vs. Signal-Noise Ratio: (a) Magnitude Gain Error, (b) Standard Deviation of (a)

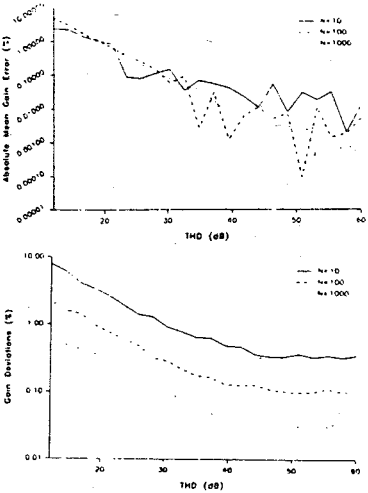


Fig.(5) Monte Carlo Simulation of the Magnitude Response vs. Total-Harmonic Distortion: (a) Magnitude Gain Error, (b) Standard Deviations of (a)

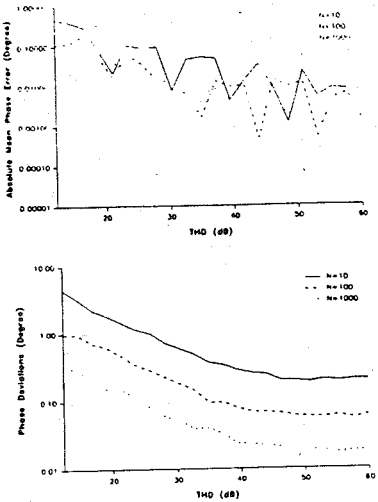


Fig.(6) Monte Carlo Simulation of the Phase Response vs. Total Harmonic Distortion: (a) Phase Error, (b) Standard Deviation of (a)

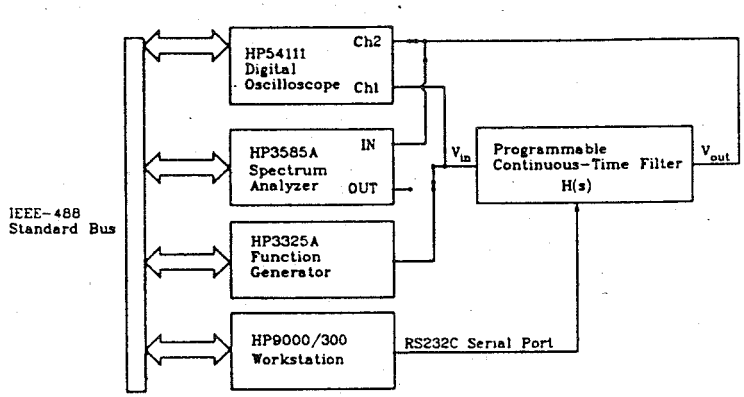


Fig.(7) Experimental Emulating Systems

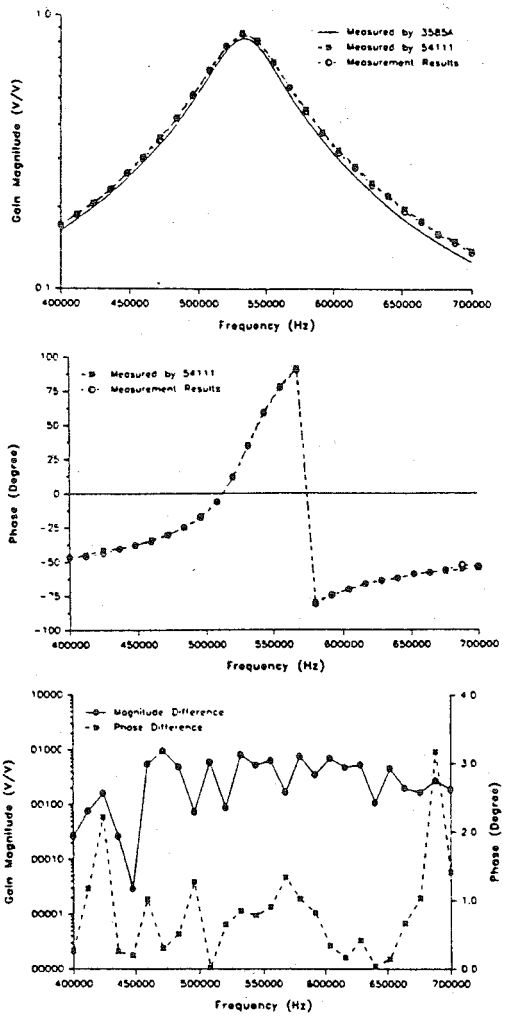


Fig.(8) Experimental Results of the Frequency Response Measurements of a 2nd-order Bandpass Filter; (a) Magnitude Response; (b) Phase Response; (c) Measurement Errors;

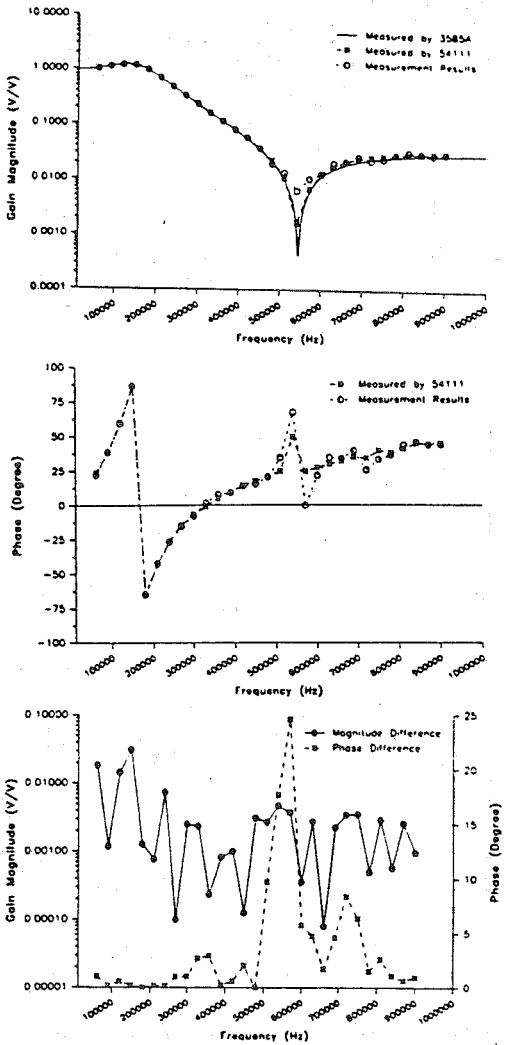


Fig.(9) Experimental Results of the Frequency Response Measurements of a 2nd-order Lowpass Notch Filter (a) Magnitude Response; (b) Phase Response; (c) Measurement Errors;